Adsorption of *p*-nitrophenol from aqueous solutions onto activated carbon fiber

Dengyong Tang, Zheng Zheng [*], Kui Lin, Jingfei Luan, Jibiao Zhang

State Key Laboratory of Pollution Control and Resource Reuse, School of the Environment,
Nanjing University, Nanjing 210093, PR China

Abstract

The adsorption of *p*-nitrophenol (PNP) onto activated carbon fiber (ACF) was investigated in simulated wastewater in a batch system to evaluate the effects of solution pH, presence of sodium chloride, adsorbent doses and temperature. It was found that PNP adsorption amount depended on pH, sodium chloride content, adsorbent doses and temperature. Langmuir and Freundlich models were applied to describe the adsorption isotherms. Freundlich model agreed with experimental data well, indicating the possibility of more than just one monomolecular layer of coverage. SEM photographs of ACF before and after adsorption revealed that it was in part with multimolecular layers of coverage on ACF surfaces. The change of free energy, enthalpy, and entropy of adsorption were also evaluated for the adsorption process. The pseudo-first-order and pseudo-second-order kinetic models were used to describe the kinetic data. The experimental data fitted very well the pseudo-second-order kinetic model. Attempts were made to desorb PNP from ACF using dilute NaOH solution and water, and desorption efficiency was obtained to the extent of 92.7% with 0.025 M NaOH and water at 368 K.
© 2006 Elsevier B.V. All rights reserved.

Keywords: Adsorption; *p*-Nitrophenol (PNP); Activated carbon fiber (ACF); Desorption

1. Introduction

There has been growing concern for public health and environmental safety over the last few decades. Introduction of toxic pollutants can have a severe impact on many organisms that live in aquatic ecosystems. *p*-Nitrophenol (PNP) is an important fine chemical intermediate, serving as a precursor of pharmaceuticals and pesticides [1]. Diesel fuel and gasoline exhaust also contain PNP that enters water body through rainwater [1,2]. PNP has been selected as one of the persistent, bioaccumulative and toxic (PBT) chemicals by the US Environmental Protection Agency [3].

Due to its harmful effects, wastewaters containing PNP have to be treated before being discharged to receiving water bodies. Many treatment technologies such as advanced oxidation processes (AOPs) [4–6], extraction [7,8], and adsorption have been developed to remove PNP from domestic and industrial wastew-aters. Adsorption is widely used because of its simple design, easy operations and relatively simple regeneration.

Although varieties of adsorbents [9–11] have been tried to remove nitrophenol from wastewaters, activated carbon (AC) [12–17] remains the most widely used adsorbent. Activated carbon fibers (ACFs) are novel adsorbents of high efficiency. The raw materials of ACFs are polyacrylonitrile fibers, viscose, phenolic resin fibers or pitch fibers, etc. They are first pyrolyzed and then activated at a temperature of 700–1000 °C in an atmosphere of steam or carbon dioxide [18]. ACFs have many favorable characteristics such as high adsorption capacities and high mass transfer rates for both adsorption and desorption, and are easier to be handled in a batch adsorber than granular and powdered AC [19]. Thus, they have received increasing attention in recent years as adsorbents for water treatment [20–23]. Furthermore, activated carbon cloths, one kind of ACFs were used as adsorbent to adsorb phenolic compounds including PNP by some researchers [24,25]. However, there is little report on thermodynamic and kinetic studies of PNP adsorption onto ACF.

The aim of this work is to study the use of ACF as an adsorbent for the removal of PNP from aqueous solutions by static batch

[*] Corresponding author. Tel.: +86 25 83593109; fax: +86 25 83707304.
E-mail address: zzheng@nju.edu.cn (Z. Zheng).

experiments. Factors affecting adsorption, such as pH, presence of NaCl, adsorbent dosage and temperature were investigated. Isotherm, thermodynamic and kinetic studies were carried out. In addition, desorption of adsorbed PNP from ACF was also studied.

2. Experimental

2.1. Adsorbent

The viscose-based ACF used in the experiments was A12 provided by the Institute of Liaoning Province Academy of Safety Science, Shenyang, China. The ACF was boiled, washed three times in distilled water and dried at 383 K for 24 h before being used as adsorbent. The specific surface area of A12 was measured with a Micrometics ASAP-2020 surface area measurement instrument (Micromeritics Instrument, Norcros, USA) following the BET method. The pH at the point of zero charge (pH$_{PZC}$) of A12 was determined by batch equilibrium method described by Babic et al [26]. The elemental analysis of A12 was obtained from a CHN-O-Rapid Elemental Analytical Instrument (Elementer, Germany). Main characteristics of A12 are summarized in Table 1.

2.2. Chemicals

All of the reagents used were A.R. grade and without further purification. Hydrochloric acid, sodium hydroxide and sodium chloride were purchased from Nanjing Chemical Reagent Plant (Nanjing, China). PNP was obtained from The Third Chemical Reagent Plant of Shanghai (Shanghai, China), and PNP solution (1000 mg/L) was prepared by dissolving required amount of PNP in distilled water in the adsorption test.

2.3. Adsorption studies

In batch adsorption experiments, certain amounts of ACF were added into several 250 mL Erlenmeyer flasks, each containing 100 mL solution (1000 mg/L PNP). And then the flasks were shaken at 150 rpm in a Constant Temperature Shaker (Shanghai Scientific Instrument Co. Ltd., China) at a pre-settled temperature for 24 h. Samples were separated by a fast filtration, and concentrations of PNP at equilibrium (C_e) were determined.

Table 1
Main characteristics of A12

Parameters	Value
Bulk density (g/cm^3)	0.04
BET surface area (m^2/g)	1413
Total pore volume (cm^3/g)	0.69
Micropore volume (cm^3/g)	0.51
Average pore width (nm)	1.95
pH$_{PZC}$	4.4
Elemental analysis (wt.%)	
C	83.32
H	1.90
O	14.78

The effect of pH on PNP adsorption onto ACF was studied by adjusting the pH of PNP solutions with dilute HCl or NaOH solution at 293 K. A PHS-2C pH meter (Shanghai Kangyi Instrument Co., China) was used to measure the pH values of the solutions. The effect of NaCl on the adsorption was also studied. Different doses of adsorbent (0.03–0.50 g) were introduced to respective 100 mL 1000 mg/L PNP solution at 293, 308 and 323 K, respectively, in order to determine adsorption isotherms and evaluate the effect of adsorbent dosage and temperature on PNP adsorption. In kinetic studies, batch experiments were conducted at different periods by adding 1.00 and 2.00 g ACF into each 500 mL solution, respectively, at pH 4.3 and 293 K.

The adsorbent phase concentrations of PNP (q_e) were calculated according to the following equation:

$$q_e = \frac{V(C_0 - C_e)}{W} \qquad (1)$$

Adsorption efficiency (AE) was calculated from following equation:

$$AE(\%) = \frac{C_0 - C_e}{C_0} \times 100 \qquad (2)$$

where C_0 and C_e are the initial and equilibrium concentrations of PNP (mg/L), respectively, V the volume of the solution (L), and W is the mass of adsorbent (g).

2.4. Scanning electron micrography of ACF before and after adsorption of PNP

A JSM-5610 scanning electron microscope (JEOL, Japan) was used to visualize the surface morphology and structure of A12 before and after adsorption of PNP.

2.5. Batch desorption

The recovery of the adsorbed material and regeneration of adsorbent are quite important in field applications of adsorption processes. It was found that the adsorption capability for adsorption of PNP onto ACF was small at high pH values. Hence, NaOH was chosen as the regeneration reagent. Ten samples of 0.40 g ACF pre-adsorbed with 100 mL solution containing 1000 mg/L PNP were added to 50 mL NaOH solutions of various concentrations (0–0.3 M) and shaken at 150 rpm in a Constant Temperature Shaker at 293 K for 2 h to determine the optimal concentration of NaOH. Studies evaluating the effect of temperature on desorption were carried out at 293, 333 and 368 K, respectively. In order to increase the desorption efficiency, the equal amount of hot water was used to rinse the ACF after dilute NaOH solution.

Desorption efficiency (DE) was calculated from the following equation:

$$DE(\%) = \frac{C_d V_d}{W_a q_e} \times 100, \qquad (3)$$

where C_d is the desorbed adsorbate concentration of desorption solution (mg/L), V_d the volume of the desorption solution (L),

W_a the mass of pre-adsorbed adsorbent (g), and q_e is the amount of adsorbate pre-adsorbed on adsorbent (mg/g).

2.6. Analysis

The concentrations of PNP were analyzed by Helious Betra UV–vis spectrometer (UK) that gave good linearity for the absorbency versus PNP concentration at its maximum absorbency wavelength 315 nm. In order to prevent pH from affecting absorbency of PNP samples, all samples were acidified by adding 0.1 M hydrochloric acid.

3. Results and discussion

3.1. Effect of pH on adsorption

The effect of pH on the adsorption is depicted in Fig. 1. When pH of the solution was lower than 4.3, the adsorption amount slightly decreased; but when pH of the solution increased to higher than 4.3, especially up to alkaline, the adsorption amount of A12 sharply decreased.

PNP is a water-soluble solid that is moderately acidic in water ($pK_a = 7.15$). When pH of the solution was lower than 4.3, almost all the PNP in solution were in molecule form, but the net charge on the surface of ACF was positive since the pH_{PZC} was found to be 4.4. There was electrostatic repulsion on the surface of ACF, which resulted in slightly decreasing the adsorption amount. At pH 4.3, the net charge on the surface of ACF was nearly zero, there was nearly no electrostatic repulsion, so the adsorption amount was maximum. While pH of the solution increased to higher than 4.3, especially up to alkaline, PNP molecules gradually ionized into PNP anions and the net charge on the surface of ACF was negative. So, electrostatic repulsions played an important role in interactions between the surface of ACF and the PNP anions. In addition, adjacent PNP anions adsorbed on the ACF surface electrostatically repelled one another [27]. Of course, there was also electrostatic repulsion on the surface of ACF. Thus, PNP anions could not pack together densely on
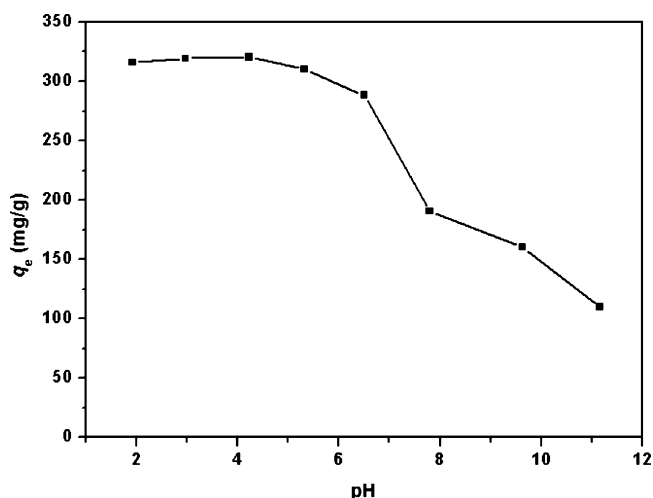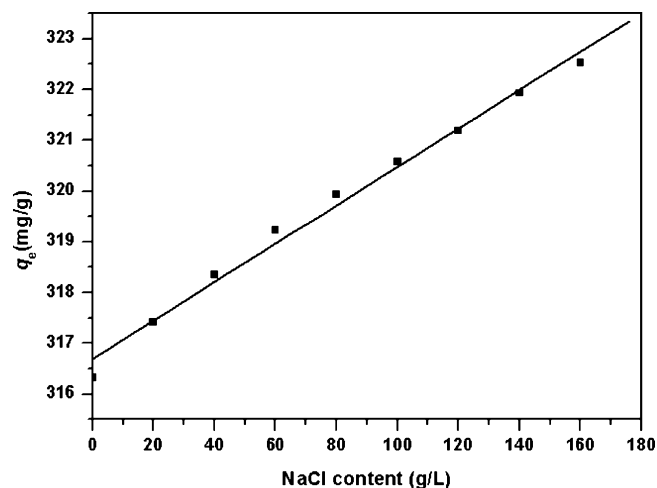
Fig. 2. Effect of NaCl on the PNP adsorption (V, 100 mL; C_0, 1000 mg/L; T, 293 K; A12 dose, 0.30 g/100 mL; pH, 4.3; agitation rate, 150 rpm; contact time, 24 h).

the surface, and the equilibrium amount of the adsorbed PNP was only modest. Similar results were observed in adsorption of phenolic compounds on activated carbon cloth [25]. This characteristic also served as the basis of using alkali to desorb ACF after adsorption. Hence, the optimal pH of solution for PNP adsorption onto ACF was determined to be 4.3.

3.2. Effect of presence of sodium chloride on adsorption

Effect of presence of sodium chloride on adsorption is depicted in Fig. 2. Under experimental conditions, PNP molecules almost existed in the molecular form. The equilibrium adsorption amount increased with increasing sodium chloride content due to the so called salting-out effect. This effect was explained by Turner and Rawling who illustrated that aqueous solubility of neutral organic compounds generally displays an inverse dependency on ionic strength [28]. Water in the presence of dissolved ions was less ordered and less compressible and the cavity volume available to accommodate PNP molecules was reduced; thus PNP solubility decreased with increasing NaCl content in the solution. The less soluble the adsorbate became, the more adsorbable it grew [29]. Experimental data supported that sodium chloride in the solution facilitated PNP adsorption on the ACF, and the equilibrium adsorption amount displayed linear dependency on NaCl content of the solution (the correlation coefficient $R^2 = 0.9902$).

3.3. Adsorption isotherms

Graphic presentations of the adsorption isotherms are shown in Fig. 3. For each isotherm, the equilibrium adsorption amount of PNP onto ACF (q_e) increased with increasing equilibrium concentration, because driving force of adsorption increased with increasing equilibrium concentration. q_e was found to decrease with increasing temperature, which indicated that PNP adsorption onto the adsorbent surface was favored at lower temperatures. This might be due to the tendency for PNP molecules
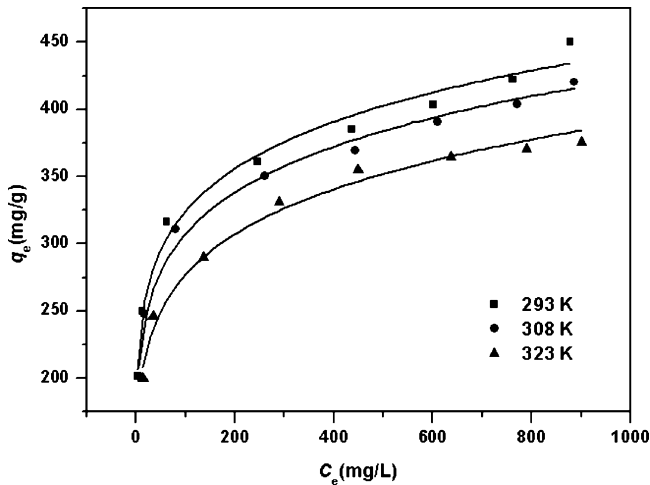
Fig. 1. Effect of pH on the PNP adsorption (V, 100 mL; C_0, 1000 mg/L; A12 dose, 0.30 g/100 mL; T, 293 K; agitation rate, 150 rpm; contact time, 24 h).

Fig. 3. Adsorption isotherms for PNP fitted by Freundlich equation (V, 100 mL; C_0, 1000 mg/L; agitation rate, 150 rpm; contact time, 24 h).

Table 2
Isotherm constants for PNP adsorption onto ACF

T (K)	Langmuir model			Freundlich model		
	q^0 (mg/g)	b	R^2	K_F	n	R^2
293	384.62	0.289	0.8557	174.52	7.435	0.9903
308	370.37	0.175	0.9061	162.26	7.215	0.9894
323	357.14	0.0828	0.9302	139.39	6.707	0.9870

to escape from the solid phase to the bulk phase with an increase in the temperature and the weakening in forces of attraction between PNP and ACF [30,31]. Furthermore, the observed phenomenon suggested that the explanation for the adsorption mechanism of PNP removal by ACF involved a physical process. So, the optimal temperature was selected to be 293 K. Also, the optimal adsorbent dosage was easily selected to be 4.00 g/L where the PNP adsorption efficiency was 98.75%.

The results were analyzed with the well-known models of Langmuir and Freundlich. Langmuir equation [32] is expressed as:

$$q_e = \frac{bq^0 C_e}{1 + bC_e},\tag{4}$$

where q_e is the amount of adsorbate taken up on adsorbent at equilibrium (mg/g), C_e the equilibrium concentration of the adsorbate in aqueous solution (mg/L), and q^0 and b are the Langmuir constants related to maximum adsorption capacity and energy of adsorption, respectively. By plotting $1/q_e$ against $1/C_e$, a straight line with a slope of $1/bq^0$ was obtained (plot not given). Freundlich equation [33] is expressed as:

$$q_e = K_F C_e^{1/n},\tag{5}$$

where q_e is the amount of adsorbate taken up on adsorbent at equilibrium (mg/g), C_e the equilibrium concentration of the adsorbate in aqueous solution (mg/L), K_F the Freundlich constant for a heterogeneous adsorbent, and n is related to the magnitude of the adsorption driving force and to the adsorbent site energy distribution. The curves were obtained by fitting the adsorption data with Eq. (5), as shown in Fig. 3.

The constants obtained according to Langmuir and Freundlich models are listed in Table 2. The correlation coefficients (R^2) for both models at different temperatures suggested that the empirical Freundlich equation was better than Langmuir equation in describing the behavior of PNP adsorption onto ACF. Langmuir model assumes uniform energies of adsorption onto the surface of adsorbent with no transmigration of adsorbate in the plane of the surface, and the adsorbed molecules have no

interaction [27]. The data obtained were not well fitted with Langmuir equation, indicating that surface energies of ACF were not uniform. Otherwise their consistence with Freundlich equation revealed that the energy distribution for the adsorption "sites" was of essentially an exponential type [27], rather than of the uniform type assumed in Langmuir isotherm. In this case, some sites were highly energetic and bound the adsorbed PNP strongly, whereas some were much less energetic and bound PNP weakly, which resulted in the possibility of more than just one monomolecular layer of coverage on the ACF surface. Thus, the adsorption of PNP in multimolecular layers was indicated in view of the experimental data.

As given in Table 2, the exponent n was larger than 1 in all cases, illuminating that the adsorption was favorable. This cohered with the characteristics of PNP adsorption isotherms shown in Fig. 3. Furthermore, n decreased with increasing temperature, which implies that the magnitude of the adsorption driving force decreased with increasing temperature. K_F also decreased with increasing temperature, which indicated that the adsorption capacity decreased when the temperature increased. Both of the Freundlich constant K_F and n showed inverse dependency on temperature, indicating the intensity of adsorption decreased with rising temperature.

3.4. Scanning electron micrography (SEM) of ACF before and after adsorption PNP

The SEM photographs of A12 before and after PNP adsorption are given in Fig. 4. Before adsorption of PNP, the surface of A12 looked relatively smooth, with several large mesopores spotted on it. During activation of A12, certain mesopore clusters were formed. Brasquet et al. also found numerous holes sized from 10 to 100 nm by SEM analyzing [34]. Provided that mesopores could hardly adsorb PNP molecules [35], PNP molecules were mostly accommodated onto micropores; hence sorts of mesopore clusters might form corresponding "holes". SEM photographs with larger magnitude revealed that the holes surfaces displayed curved planes, which might be ascribed to heterogeneous energy distribution of the activated adsorption sites on ACF surface. The observed phenomenon also provided evidence for the discussed conclusion that the adsorption process involved multimolecular layers of coverage on ACF surface.

3.5. Thermodynamic parameters

The thermodynamic parameters for the adsorption process, $\Delta H°$ and $\Delta S°$, were evaluated using the equation [36,37]:
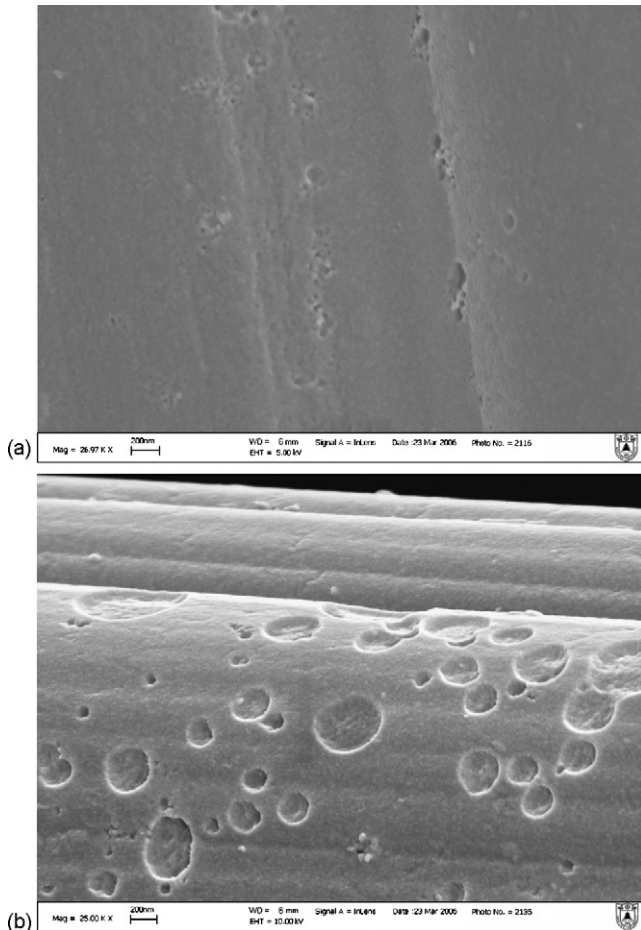
(a)

(b)

Fig. 4. The SEM photographs of A12 (a) before PNP adsorption (200 nm) and (b) after PNP adsorption (200 nm).

$$\ln C_{\mathrm{e}} = \left(\frac{\ln q_{\mathrm{e}} - \Delta S^{\circ}}{R} \right) + \frac{\Delta H^{\circ}}{R} \frac{1}{T}, \qquad (6)$$

where ΔS° and ΔH° are the entropy (J/(mol K)) and enthalpy (J/mol) change of adsorption, respectively, R the universal gas constant (8.314 J/(K mol)), and T is the absolute temperature (K). At different temperatures (293–323 K), the corresponding C_{e} values for different fixed q_{e} were calculated by the well-fitted Freundlich isotherms. Thus, ΔH° and ΔS° were obtained from the slope and intercept of the line plotted by $\ln C_{\mathrm{e}}$ versus $1/T$, respectively, as shown in Fig. 5. The correlation coefficients (R^2) for the linear equations were 0.9618, 0.9646, and 0.9673, respectively. ΔS° and ΔH° values were used to compute ΔG° from the Gibbs equation ($\Delta G^{\circ} = \Delta H^{\circ} - T\Delta S^{\circ}$) at constant temperatures. Related thermodynamic parameters are listed in Table 3.

As given in Table 3, the enthalpy changes (ΔH°) were negative and the absolute values were lower than 40 kJ/mol, indicating that the adsorption is an exothermic physical process [38]. In addition, the enthalpy change was found to be dependent of the equilibrium adsorption amount, which was due to the heterogeneity of the adsorption sites on ACF surface. In principle, PNP molecules were first adsorbed at the more active sites, which gave relatively high enthalpy change. Subsequently, the less active sites were occupied and/or multimolecular layers of
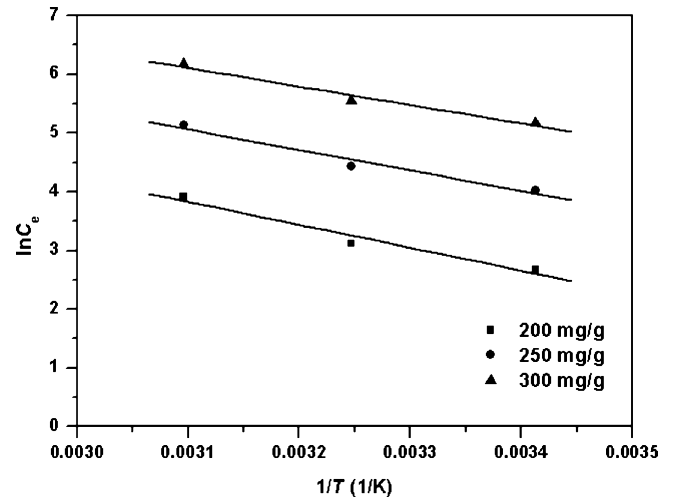

Fig. 5. Plot of ln C_{e} vs. $1/T$ for estimation of thermodynamic parameters for the adsorption of PNP onto ACF.

coverage occurred at the more active sites. This consequently led to the decreased enthalpy change with the increase of equilibrium adsorption amount.

The adsorption entropy changes (ΔS°) were less than zero, which accorded with the fact that the mobility of adsorbates on adsorbent surface becomes more restricted as compared with that of those in solution. Besides, it was shown that ΔS° increased with the increase in equilibrium adsorption amount.

The free energy changes (ΔG°) were less than zero, demonstrating that the discussed adsorption is a spontaneous process. While the equilibrium adsorption amount increased, the absolute value of ΔG° decreased correspondingly, which indicated the decrease in adsorption impetus. On the same equilibrium adsorption amount condition, the absolute values of ΔG° decreased with increasing temperature. Both of the phenomena suggested that on the condition of larger equilibrium adsorption amount and higher temperature, the reverse process of adsorption–desorption could be easily carried out.

3.6. Adsorption kinetics

Plots of adsorption amount versus time are shown in Fig. 6. The equilibrium adsorption amount of 2.00 and 4.00 g ACF/L were 354.86 and 247.85 mg/g, respectively. It was also shown that 2.00 and 4.00 g ACF/L reached 77.55% and 84.78% of respective equilibrium adsorption amount after 3 min.

In order to investigate the mechanism of adsorption, the pseudo-first-order and pseudo-second-order equations are

Table 3
Thermodynamic data for adsorption of PNP onto ACF evaluated at different equilibrium adsorption amounts and different temperatures

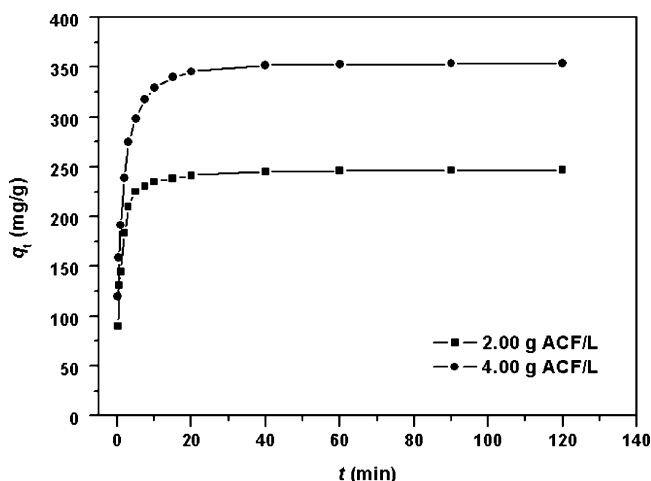| q_{e} (mg/g)	ΔH° (kJ/mol)	ΔS° (J/(K mol))	ΔG° (kJ/mol)		
			293 K	308 K	323 K
200	−36.74	−89.12	−10.63	−9.29	−7.95
250	−32.50	−86.70	−7.10	−5.80	−4.50
300	−29.05	−84.74	−4.22	−2.95	−1.68

Fig. 6. Plot of q_t vs. time for the adsorption of PNP onto ACF at various ACF doses (C_0, 1000 mg/L; V, 500 mL; T, 293 K; agitation rate, 150 rpm).

Fig. 7. Pseudo-second-order kinetic plots for the adsorption of PNP onto ACF at various adsorbent doses.

applied to model the kinetics of PNP adsorption onto ACF. The pseudo-first-order rate expression of Langergren [39] is presented as:

$$\ln(q_e - q_t) = \ln q_e - k_1 t, \tag{7}$$

And the pseudo-second-order kinetic model [39,40] is expressed as:

$$\frac{t}{q_t} = \frac{1}{k_2 q_e^2} + \frac{1}{q_e} t, \tag{8}$$

where q_e is the amount of PNP adsorbed on adsorbent at equilibrium (mg/g), q_t the amount of PNP adsorbed at various times t (mg/g), k_1 the pseudo-first-order rate constant for the adsorption process (min^{-1}) and k_2 is the rate constant of pseudo-second-order adsorption (g/(mg min)).

The slopes and intercepts of plots of $\ln(q_e - q_t)$ versus t were obtained to determine the first-order rate constant k_1 and equilibrium adsorption amount q_e (plots not shown). The calculated results and corresponding correlation coefficients (R^2) are listed in Table 4. The correlation coefficients for the first-order kinetic model at different ACF doses were relatively low and the calculated q_e values obtained from the first-order kinetic model failed to match the experimental q_e values, together indicating that the adsorption of PNP onto ACF was not a first-order reaction.

The slopes and intercepts of plots of t/q_t versus t were obtained to calculate the second-order rate constant k_2 and q_e. The straight lines in Fig. 7 shows a good agreement of experimental data with the second-order kinetic model at different ACF doses. Computed results obtained from the second-order kinetic
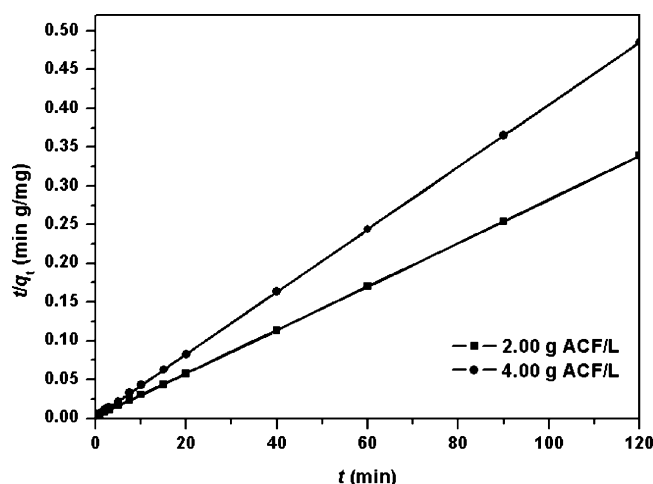
model are listed in Table 4. The correlation coefficients for the second-order kinetic model at different ACF doses equaled to 1.000. Moreover, the calculated q_e values remained consistent with the experimental data. These indicated that the adsorption system studied obeyed the second-order kinetic model. Similar results were also obtained in adsorption of basic dyes on pumice and biosorption of remazol black B on biomass [40,41].

3.7. Desorption studies

The amount of PNP desorbed as a function of NaOH concentration is shown in Fig. 8. For 0.025 mol/L NaOH solution, where the NaOH dosage equaled to 1.76 times the amount of the theoretical NaOH dosage, the desorption efficiency was 60.22%. During the desorption process, the formation of sodium salt of PNP facilitated the desorption of PNP from the ACF surfaces. The desorption efficiency was 61% using 0.15 M NaOH solution to desorb phenol from activated carbon [42], where the NaOH dosage was 150 times as many as the theoretical NaOH dosage. Once NaOH concentration was more than 0.025 mol/L, however, desorption efficiency slightly decreased. This phenomenon could be attributed to the decrease in the strength of repulsion between PNP anions and surface of ACF and the adjacently adsorbed PNP anions on ACF surfaces with more Na$^+$ presented in aqueous solution, allowing more PNP anions on the surface [43]. Hence, PNP adsorbed on ACF was ready to be desorbed by NaOH solution, and the optimal concentration of NaOH for desorption was 0.025 mol/L.

The PNP desorption curves using 0.025 mol/L NaOH at different temperatures are shown in Fig. 9. At 293 K, desorption

Table 4
Kinetic parameters for the adsorption of PNP onto ACF at different adsorbent doses

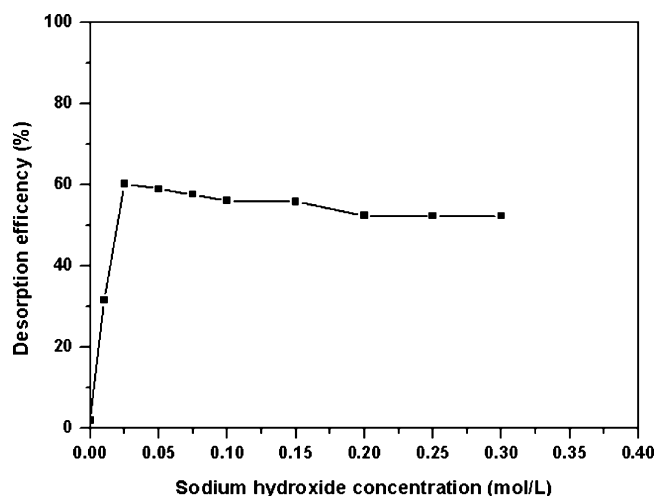| Parameters	$q_{e,exp}$ (mg/g)	Pseudo-first-order (0–3 min)			Pseudo-second-order (0–120 min)		
		k_1 (min^{-1})	$q_{e,cal}$ (mg/g)	R^2	k_2 (g/(mg min))	$q_{e,cal}$ (mg/g)	R^2
2.00 g ACF/L	355.01	0.4386	279.69	0.933	0.00356	357.14	1.000
4.00 g ACF/L	247.85	0.5549	191.20	0.944	0.00695	250.00	1.000

Fig. 8. Desorption efficiency of PNP from ACF by NaOH solution after pre-adsorbing 1000 mg/L PNP solution for 24 h (*V*, 50 mL; ACF dose, 0.40 g; *T*, 293 K; agitation rate, 150 rpm; contact time, 2 h).

equilibrium was achieved within 5 min up to the desorption efficiency of 60.22%; at 333 K, within 3 min up to the desorption efficiency of 68.13%; and at 368 K, within 2 min up to 78.2%. Desorption efficiency increased with increasing temperature, while the time for achieving desorption equilibrium decreased with the increase in temperature. The reason was that the solubility of sodium salt of PNP, as well as the mobility of PNP anions, increased with increasing temperature, which facilitated the desorption process. So the optimal temperature for desorption was 368 K.

In order to increase the desorption efficiency, equal amount of water at 368 K was used to rinse the ACF for 2 min after 0.025 M NaOH solution desorption. Thus the total desorption efficiency of adsorbed PNP reached up to 92.7%. Therefore, 0.025 mol/L NaOH solution and water at 368 K was used as the optimal desorption reagent.
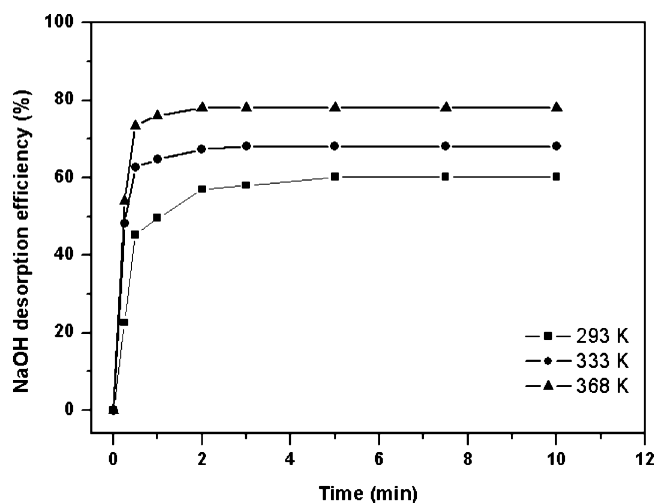
4. Conclusions

This study investigated the behavior and mechanism of the adsorption of PNP from aqueous solutions onto ACF, coupled with the optimal conditions for desorption of adsorbed PNP from ACF. The adsorption was found to depend on pH, sodium chloride content, adsorbent doses, and temperature. At initial PNP concentration of 1000 mg/L and on the optimal condition (pH 4.3, ACF dose 4.00 g/L, temperature 293 K), the adsorption efficiency was 98.75%, and the equilibrium adsorption amount was 247.85 mg/g. Freundlich equation was better than Langmuir equation in describing the adsorption equilibrium data. SEM photographs of ACF before and after adsorption revealed that the adsorption is in part with multimolecular layers of coverage on the ACF.

The enthalpy changes for the adsorption (ΔH°) were all negative and their absolute values were less than 40 kJ/mol; hence the adsorption are controlled an exothermic and mainly physical process. The adsorption entropy changes (ΔS°) were all less than zero, conforming to the fact that the mobility of adsorbates on adsorbent surface becomes more restricted compared with that of those in solution. The free energy changes (ΔG°) were all less than zero, demonstrating that the studied adsorption is a spontaneous process.

Within 3 min, the uptake of PNP reached 84.78% of equilibrium adsorption amount at the adsorbent dose of 4.00 g/L. The pseudo-second-order kinetic model fits very well with the dynamic experimental data.

It only took 2 min to achieve desorption equilibrium with desorption efficiency of 92.7% by using 0.025 M NaOH and water at 368 K. 0.025 mol/L NaOH solution and water is efficient for desorption of PNP from ACF.

References

[1] A. Boehncke, G. Koennecker, I. Mangelsdorf, A. Wibbertmann, Mononitrophenols, concise international chemical assessment document 20 (2000). Available from: http://www.who.int/ipcs/publications/cicad/en/cicad20.pdf.
[2] J. Tremp, P. Mattrel, S. Fingler, W. Giger, Phenols and nitrophenols as tropospheric pollutants: emissions from automobile exhausts and phase transfer in the atmosphere, Water Air Soil Pollut. 68 (1993) 113–123.
[3] US Environmental Protection Agency, Release and pollution prevention report, 2000.
[4] O. Gimeno, M. Carbajo, F.J. Beltran, F.J. Rivas, Phenol and substituted phenols AOPs remediation, J. Hazard. Mater. B119 (2005) 99–108.
[5] M. Ksibi, A. Zemzemi, R. Boukchina, Photocatalytic degradability of substituted phenols over UV irradiated TiO₂, J. Photochem. Photobiol. A: Chem. 159 (2003) 61–70.
[6] P. Canizares, J. Lobato, R. Paz, M.A. Rodrigo, C. Saze, Electrochemical oxidation of phenolic wastes with boron-doped diamond anodes, Water Res. 39 (2005) 2687–2703.
[7] S.W. Peretti, C.J. Tompkins, J.L. Goodall, A.S. Michaels, Extraction of 4-nitrophenol from 1-octanol into aqueous solution in a hollow fiber liquid contactor, J. Membr. Sci. 195 (2001) 193–202.

Fig. 9. Effect of temperature on the NaOH desorption of PNP from ACF (NaOH concentration, 0.025 mol/L; *V*, 200 mL; ACF dose, 1.60 g; agitation rate, 150 rpm).

[8] J. Luan, A. Plaisier, Study on treatment of wastewater containing nitrophenol compounds by liquid membrane process, J. Membr. Sci. 229 (2004) 235–239.

[9] A. Li, Q. Zhang, G. Zhang, J. Chen, Z. Fei, F. Liu, Adsorption of phenolic compounds from aqueous solutions by a water-compatible hypercrosslinked polymeric adsorbent, Chemosphere 47 (2002) 981–989.

[10] T. Sismanoglu, S. Pura, Adsorption of aqueous nitrophenols on clinoptilolite, Colloids Surf. A 180 (2001) 1–6.

[11] M. Akcay, G. Akcay, The removal of phenolic compounds from aqueous solutions by organophilic bentonite, J. Hazard. Mater. B113 (2004) 189–193.

[12] A. Wolborska, Adsorption on activated carbon of *p*-nitrophenol from aqueous solution, Water Res. 23 (1989) 85–91.

[13] C. Moreno-Castilla, J. Rivera-Utrilla, M.V. Lopez-Ramon, F. Carrasco-Marin, Adsorption of some substituted phenols on activated carbons from a bituminous coal, Carbon 33 (1995) 845–851.

[14] A.A.M. Daifullah, B.S. Girgis, Removal of some substituted phenols by activated carbon obtained from agriculture waste, Water Res. 32 (1998) 1169–1177.

[15] S. Haydar, M.A. Ferro-Garcia, J. Rivera-Utrilla, J.P. Joly, Adsorption of *p*-nitrophenol on an activated carbon with different oxidations, Carbon 41 (2003) 387–395.

[16] J.M. Chern, Y.W. Chien, Adsorption of nitrophenol onto activated carbon: isotherms and breakthrough curves, Water Res. 36 (2002) 647–655.

[17] S. Nouri, F. Haghseresh, Adsorption of *p*-nitrophenol in untreated and treated activated carbon, Adsorption 10 (2004) 79–86.

[18] J.P. Donnet, R.C. Bansal, Carbon Fibers, 2nd ed., Marcel Dekker, New York, USA, 1990.

[19] M. Suzuki, Activated carbon fiber: fundamentals and applications, Carbon 32 (1994) 577–586.

[20] C. Brasquet, P. Le Cloriec, Adsorption onto activated carbon fibers: application to water and air treatments, Carbon 35 (1997) 1307–1313.

[21] I. Martin-Gulloan, R. Font, Dynamic pesticide removal with activated carbon fibers, Water Res. 35 (2001) 516–520.

[22] P.A. Quinlivan, L. Li, D.R.U. Knappe, Effects of activated carbon characteristics on the simultaneous adsorption of aqueous organic micropollutants and natural organic matter, Water Res. 39 (2005) 1663–1673.

[23] Y. Miyake, A. Sakoda, H. Yamanashi, H. Kaneda, M. Suzuki, Activated carbon adsorption of trichloroethylene (TCE) vapor stripped from TCE-contaminated water, Water Res. 37 (2003) 1852–1858.

[24] C. Brasquet, E. Subrenat, P. Le Cloirec, Removal of phenolic compounds from aqueous solution by activated carbon cloths, Water Sci. Technol. 39 (1999) 201–205.

[25] E. Ayranci, O. Duman, Adsorption behaviors of some phenolic compounds onto high specific area activated carbon cloth, J. Hazard. Mater. B124 (2005) 125–132.

[26] B.M. Babic, S.K. Milonjic, M.J. Polovina, B.V. Kaludierovic, Point of zero charge and intrinsic equilibrium constants of activated carbon cloth, Carbon 37 (1999) 477–481.

[27] D.O. Cooney, Adsorption Design for Wastewater Treatment, Lewis Publishers, USA, 1999.

[28] A. Turner, M.C. Rawling, Influence of salting out on the sorption of neutral organic compounds in estuaries, Water Res. 35 (2001) 4379–4389.

[29] E.G. Furuya, H.T. Chang, Y. Miura, K.E. Noll, A fundamental analysis of the isotherm for the adsorption of phenolic compounds on activated carbon, Sep. Purif. Technol. 11 (1997) 69–78.

[30] W.T. Tsai, C.W. Lai, K.J. Hsien, Adsorption kinetics of herbicide paraquat from aqueous solution onto activated bleaching earth, Chemosphere 55 (2004) 829–837.

[31] D. Singh, Effect of different factors on the adsorption of phosphamidon on two different types of Indian soil, Adsorpt. Sci. Technol. 16 (1998) 583–594.

[32] V.K. Gupta, I. Ali, V.K. Saini, Removal of chlorophenols from wastewater using red mud: an aluminum industry waste, Environ. Sci. Technol. 38 (2004) 4012–4018.

[33] S.H. Lin, C.Y. Huang, Adsorption of BTEX from aqueous solution by macroreticular resins, J. Hazard. Mater. A70 (1999) 21–37.

[34] C. Brasquet, B. Rousseau, H. Estrade-Szwarckopf, P. Le Cloirec, Observation of activated carbon fibers with SEM and AFM correlation with adsorption data in aqueous solution, Carbon 38 (2000) 407–422.

[35] Z. Ryu, J. Zheng, M. Wang, B. Zhang, Characterization of pore size distributions on carbonaceous adsorbents by DFT, Carbon 37 (1999) 1257–1264.

[36] E. Tutem, R. Apak, C.F. Unal, Adsorptive removal of chlorophenols from water by bituminous shale, Water Res. 32 (1998) 2315–2324.

[37] S.S. Gupta, K.G. Bhattacharyya, Adsorption of Ni(II) on clays, J. Colloid Interf. Sci. 295 (2006) 21–32.

[38] M. Karaa, H. Yuzera, E. Sabah, Adsorption of cobalt from aqueous solutions onto sepiolite, Water Res. 37 (2003) 224–232.

[39] Y.S. Ho, G. McKay, Sorption of dye from aqueous solution by peat, Chem. Eng. J. 70 (1998) 115–124.

[40] F. Akbal, Adsorption of basic dyes from aqueous solution onto pumice powder, J. Colloid Interf. Sci. 286 (2005) 455–458.

[41] Z. Aksu, S. Tezer, Equilibrium and kinetic modelling of biosorption of remazol black B by *Rhizopus arrhizus* in a batch system: effect of temperature, Process Biochem. 36 (2000) 431–439.

[42] B. Ozkaya, Adsorption and desorption of phenol on activated carbon and a comparison of isotherm models, J. Hazard. Mater. B129 (2006) 158–163.

[43] V.L. Snoeyink, W.J. Weber Jr., H.B. Mark Jr., Sorption of phenol and nitrophenol by activated carbon, Environ. Sci. Technol. 3 (1969) 918–926.